OXFORD

Social Cognitive and Affective Neuroscience, 2022, **17**, 1007–1020

DOI: https://doi.org/10.1093/scan/nsac025
Advance Access Publication Date: 26 March 2022
Original Manuscript

Neural connectivity underlying adolescent social learning in sibling dyads

Christy R. Rogers,[1] Cassidy M. Fry,[2] Tae-Ho Lee,[3] Michael Galvan,[1] Kathleen M. Gates,[4] and Eva H. Telzer[4]

[1]Department of Human Development and Family Sciences, Texas Tech University, Lubbock, TX 79409, USA
[2]Department of Human Development and Family Studies, Pennsylvania State University, State College, PA 16801, USA
[3]Department of Psychology, Virginia Polytechnic Institute and State University, Blacksburg, VA, 24061-0131, USA
[4]Department of Psychology and Neuroscience, University of North Carolina at Chapel Hill, Chapel Hill, NC 27599, USA
Correspondence should be addressed to Christy Rogers, Department of Human Development and Family Sciences, Texas Tech University, 1301 Akron Ave, Lubbock, TX 79415, USA. E-mail: christy.rogers@ttu.edu.

Abstract

Social learning theory posits that adolescents learn to adopt social norms by observing the behaviors of others and internalizing the associated outcomes. However, the underlying neural processes by which social learning occurs is less well-understood, despite extensive neurobiological reorganization and a peak in social influence sensitivity during adolescence. Forty-four adolescents (Mage = 12.2 years) completed an fMRI scan while observing their older sibling within four years of age (Mage = 14.3 years) of age complete a risky decision-making task. Group iterative multiple model estimation (GIMME) was used to examine patterns of directional brain region connectivity supporting social learning. We identified group-level neural pathways underlying social observation including the anterior insula to the anterior cingulate cortex and mentalizing regions to social cognition regions. We also found neural states based on adolescent sensitivity to social learning via age, gender, modeling, differentiation, and behavior. Adolescents who were more likely to be influenced elicited neurological up-regulation whereas adolescents who were less likely to be socially influenced elicited neurological down-regulation during risk-taking. These findings highlight patterns of how adolescents process information while a salient influencer takes risks, as well as salient neural pathways that are dependent on similarity factors associated with social learning theory.

Key words: adolescence; fMRI; social learning; siblings; risk taking

Adolescents develop behaviors and attitudes associated with risk taking through modeling the actions of other individuals (e.g. Whiteman *et al.*, 2014). According to social learning theory, adolescents learn social norms by observing the behaviors of others and internalizing the associated outcomes (Bandura, 1977; Akers *et al.*, 1979). Adolescents are especially sensitive to social cues as a result of rapid biopsychosocial development and dynamic shifts in environmental contexts during adolescence (Gardner and Steinberg, 2005; Blakemore and Robbins, 2012; Perino *et al.*, 2016; Casey *et al.*, 2019), including influence from parents, peers and siblings (Telzer *et al.*, 2018). This growing literature suggests that adolescent learning is dependent on their social context such that adolescents will change their perception of risk and prosocial attitudes based on the opinions endorsed by peers (Knoll *et al.*, 2017; Foulkes *et al.*, 2018). While social influence peaks during adolescence (Blakemore and Mills, 2014), as well as extensive neurobiological reorganization of the adolescent brain during puberty (Casey *et al.*, 2019), the underlying neural processes by which social learning occurs is less well-understood.

Developmental neuroscience research has identified brain regions associated with decision-making and learning during adolescence. In particular, a recent meta-analysis identified the ventral striatum (VS), anterior insula (AI) and medial prefrontal cortex (mPFC) as key brain regions involved in decision-making across social contexts (van Hoorn *et al.*, 2019). Indeed, the VS is involved in reward processing, particularly in the presence of social cues (Chein *et al.*, 2011; Perino *et al.*, 2016), the mPFC is implicated in regulation and value-based decision-making (Qu *et al.*, 2015; Blankenstein *et al.*, 2018) and the AI integrates feedback from affective and cognitive regions to guide decision-making and learning processes (Jones *et al.*, 2014; Op de Macks *et al.*, 2018). Regions implicated in salience detection during context-dependent decision-making may also underlie social learning, including the amygdala, which is involved in affective processing (Mather *et al.*, 2004), and the anterior cingulate cortex (ACC), which is involved in decision-making during reward-dependent processing (Jones *et al.*, 2011), particularly in processing social information during learning (Kendal *et al.*, 2018).

Received: 15 June 2021; **Revised:** 7 February 2022; **Accepted:** 23 March 2022

Additional social cognition regions, such as the temporoparietal junction (TPJ), superior temporal sulcus (STS), temporal poles and precuneus, are involved in mentalizing during decision-making in adolescence (van Hoorn *et al.*, 2014; Welborn *et al.*, 2016). Finally, adolescent decision-making across various social contexts includes receiving visual information, such as goal-oriented actions. Error-processing of incorrect actions associates with activation in the intraparietal sulcus (IPS) and may be partially responsible for interpreting intentions in peer actions (Hamilton and Grafton, 2006), and the fusiform face area (FFA) is involved in visual attention given to people relative to other objects and may support observational processes being receptive to social cues (Schultz *et al.*, 2003; Rhodes *et al.*, 2004).

Although these neuroscience models have examined key regions associated with social influence on adolescent learning and decision-making, they typically rely on group trends despite research suggesting a large degree of individual variability in adolescent risky decision-making (Silverman *et al.*, 2015; Blankenstein *et al.*, 2018). Further, prior work typically examines these brain regions in isolation using univariate brain activation rather than as a network of functional connectivity between brain regions. Using social learning theory as a guiding framework, identifying functional pathways in the adolescent brain that underlie social learning during risk taking may contribute to our understanding of context-specific behavioral outcomes during adolescence. Using group iterative multiple model estimation (GIMME; Gates and Molenaar, 2012), we can utilize variability within and across individuals to reliably examine patterns of directional brain region connectivity that support social learning. In addition, GIMME estimates functional connectivity across a task such that previous time points are controlled for to test directionality (Lane and Gates, 2017), which allows us to capture change in neural connectivity underlying the complex processes of social learning. Using sophisticated tools such as GIMME provides the opportunity to accurately identify social learning connectivity maps, as well as account for variability in individuals, and time as the process of social learning unfolds.

Individuals are selective in who they attend to in the context of social learning (Kendal *et al.*, 2018), suggesting that the characteristics of a model, and the way in which adolescents perceive a model, likely influences the degree to which adolescents learn from others. Sibling relations provide a fruitful opportunity to examine social learning given their extensive time spent in joint activities and observing one another in shared environments (Tucker *et al.*, 2001; Buchanan *et al.*, 2009). Previous literature on social proximity during development has identified greater engagement in health-risk behaviors for adolescents who maintain close ties with social agents who model risky behaviors (Ennett *et al.*, 2006; Christakis and Fowler, 2013). In a peer network, social proximity and status may determine the direction of influence, which tends to be multidirectional as adolescents observe and learn from one another (Meldrum *et al.*, 2012). However, for siblings, the direction of influence tends to be unidirectional. Due to age and experience, older siblings generally have a unique position of power relative to a younger sibling and are used as a source of reference by younger siblings when navigating their own personal development (Furman and Buhrmester, 1985). This imbalance of power can create an asymmetric effect by which younger siblings perceive closer social proximity to their older sibling(s) than vice versa, and, thus, younger siblings are more readily susceptible to influence (Magee and Smith, 2013), especially in same-sex dyads (Whiteman *et al.*, 2011). Indeed, older and younger siblings show similar behavior in their substance use, risky sexual behaviors and delinquency (Stormshak *et al.*, 2004; Whiteman *et al.*, 2014; Samek *et al.*, 2018). Moreover, we have shown in this same sample that similarity in siblings' risky (and cautious) behavior increases following observation of older sibling behavior during adolescence (Rogers *et al.*, 2021). Furthermore, sibling risk-taking behavior predicts adolescent risk taking above and beyond that of parents and peers (Duncan *et al.*, 1996; Pomery *et al.*, 2005; Yurasek *et al.*, 2018), highlighting the unique position of siblings as models in adolescent social learning. Of note, the extent to which sibling influence plays a role in adolescent behavior becomes stronger among sibling dyads with increased characteristic similarities such as being closer in age (Feinberg and Hetherington, 2000; Samek and Rueter, 2011), same sex (Rowe and Gulley, 1992; Slomkowski *et al.*, 2001) and when older siblings are perceived as a valuable model and younger siblings do not try to differentiate from them (Whiteman *et al.*, 2007). When characteristically similar in age or sex or when individuals hold favorable views of their older sibling, adolescents may be more inclined to adopt observed sibling behavioral patterns during circumstances involving risk or uncertainty (D'Amico and Fromme, 1997; Loewenstein *et al.*, 2001; Slomkowski *et al.*, 2001).

Developmental neuroscience has begun examining functional connectivity between brain regions during social cognition in adolescence (McCormick *et al.*, 2018), and these neural pathways may provide unique information about how social learning differs across different types of dyads. Thus, we investigated the functional brain connections that underlie adolescent social learning from older siblings, particularly based on sibling age spacing, sex composition of the sibling dyad, adolescent perception of older sibling modeling, adolescent differentiation from their older sibling modeling and change in adolescents' behavior after observing their older sibling. To capture social learning, adolescents completed an functional magnetic resonance imaging (fMRI) scan while they observed their older siblings complete a risky decision-making task, the Yellow Light Game (YLG; Op de Macks *et al.*, 2018). GIMME (Gates and Molenaar, 2012) was conducted to identify group network connectivity maps of social learning. In addition, five confirmatory GIMME analyses were conducted to create subgroup connectivity maps to identify differences between adolescents who are more likely to be influenced (i.e. high-influence subgroup) and those who are less likely to be influenced (i.e. low-influence subgroup) based on social learning factors: demographics that suggest higher probability of influence (i.e. age spacing and sex composition), self-reported modeling and differentiation that suggest higher probability of influence and actual influence (i.e. change in task behavior). Given that these social learning factors likely distinguish the neurobiological processing adolescents exhibit, we proposed that significant paths would emerge differentially between high-influence subgroups (e.g. closer in age siblings) compared to low-influence subgroups (e.g. further in age siblings), as well as between different sources of influence (e.g. closer in age versus self-report influence).

Methods

Participants

Participants included 44 families with a focal adolescent (M_{age} = 12.2 years, range = 10.6–14.3; 23 females) and their older sibling (M_{age} = 14.6 years, range = 12.7–17.1; 20 females). Inclusion criteria included being 10–14 years old, with an older sibling

Table 1. Demographics of adolescent ethnicity, sex composition of sibling dyads, family total income, parental education and parental marital status ($n = 44$)

Variables	n (%)
Adolescent ethnicity	
Latino/Hispanic	5 (11.4%)
African American/Black	4 (9.1%)
Asian American/Pacific Islander	1 (2.3%)
Caucasian/White	31 (70.4%)
Multiethnic	3 (6.8%)
Sex composition of sibling dyads	
Female–female	9 (20.5%)
Male–male	10 (22.7%)
Female–male	14 (31.8%)
Male–female	11 (25.0%)
Total family income	
< $45 000	3 (6.8%)
$45 000—$74 999	11 (25.0%)
$75 000—$99 999	13 (29.5%)
$100 000—$150 000	11 (25.0%)
> $150 000	6 (13.6%)
Participating parent education	
Some high school	1 (2.3%)
High school diploma	1 (2.3%)
Some college	6 (13.6%)
Associate's degree	6 (13.6%)
Bachelor's degree	12 (27.3%)
Some graduate school	3 (6.8%)
Master's degree (e.g. M.A., M.SW.)	12 (27.3%)
Professional degree (e.g. M.D., Ph.D.)	3 (6.8%)
Participating parent marital status	
Divorced or never married	3 (6.8%)
Married	34 (77.3%)
Divorced and remarried	7 (15.9%)

within 4 years of age (*M* age spacing = 2.43 years, range = 1.19–4.29). Criteria for siblingship included that the older sibling lived in the home for the duration of the focal adolescent's life as a sibling. Family demographic information is displayed in Table 1. Both adolescent participants ($n = 88$) from each family were screened for and free from MRI contraindications, psychological disorders, learning disabilities and neurological-altering medications. One additional sibling dyad was excluded from analyses because one adolescent did not complete the scan due to claustrophobia.

Both older and younger siblings completed an fMRI scan and questionnaires at the session. Older siblings first completed one run of the risky decision-making task (described below) during an fMRI scan, during which the screen was recorded using a computer screen recording program (Bandicam, Seoul, Korea). The recording showed only the screen from the participant's point of view. Focal adolescents then completed an fMRI scan, during which they completed two runs of the same task, then observed the recording of their older sibling's performance on the task, which was the social learning run of interest in this study, and then completed the task one more time. Although participants were informed during the consenting process that their performance might be shared with family members, older siblings were not made explicitly aware that their task was being recorded during the session. However, focal adolescents were informed prior to the session that their older sibling's performance had been recorded, and they were explicitly instructed during the social learning condition to not press any buttons but to watch how their sibling played the game. The same participants and task was used in Rogers *et al.* (2021), which utilized the first and last runs of the task to examine neural similarity in sibling dyads during risky decision-making. All participants provided written assent with parental consent in accordance with the institutional review board.

Risky decision-making task

Older and younger siblings completed the YLG (Op de Macks *et al.*, 2018), a risky decision-making task adapted from the Stoplight task (Chein *et al.*, 2011), to examine adolescent social learning of risk taking from older siblings. The YLG paradigm and sequence of rounds are displayed in Figure 1. This task serves as a model of unpredictable risk and offers participants the choice between risky and safe decisions, which more closely resembles real-life decision-making. Participants completed a virtual driving course in which a car from the driver's point of view is driven along a straight road with several intersections. Each intersection is controlled by a stoplight that turns yellow as the car approaches, signaling the need for a decision. Participants were instructed to complete the course as quickly as possible by choosing to either stop or go at each intersection. Choosing to go through the intersection is the fastest option and results in no delay if successful and is paired with a positive chiming sound and a blue visual tilde cue. However, if a go decision results in a crash, the car is delayed 5 s and is paired with a honking car sound, crash noise and broken windshield cue. Choosing to stop results in a 2.5-s delay and is paired with either an approaching car that honks or an empty intersection. Importantly, any cars that approach the intersection are not visible to the participant until after they have made their decision.

Participants were trained on the YLG by playing two full rounds before the scan to improve engagement and eliminate learning effects, which was successful in this sample (see Rogers *et al.*, 2021). Participants received warning cues if they did not choose to go or stop, which included a red X cue, error noise and a 5-s delay, which prompted engagement in the task. The no-response trials resulted in a 1-s delay during the actual scan, but participants were not explicitly prompted about this change. Each run of the task included 30 intersections and lasted for approximately 4 min. The probability of a car passing through the intersection was kept constant at 50%, and the perceived distance to the yellow light varied between 200 and 250 feet. Participants were not made explicitly aware of the probability of crashing. The timing and onset of the yellow light were 1.5 s after the previous trial and 200 or 250 ms prior to the onset of the red light. All runs of the YLG were different from one another in the onset of yellow and red lights, as well as the intersections in which cars approached the intersection.

Subgrouping measures

Adolescents were separated into two subgroups (i.e. high influence versus low influence) across five measures based on how likely sibling characteristics and dynamics were to influence adolescents. This resulted in a total of 10 overlapping subgroups. For instance, an individual could be considered to be in the 'high-influence' subgroup based on closeness in age but in the 'low-influence' subgroup based on sex composition (see Figure 2 for characteristics and *n*s of each subgroup). The distribution of adolescents who belonged to a given number of the five high-influence subgroups across the five sets of analyses was normally distributed such that being a member in high-influence subgroups varied from 0 to 5 (0 high-influence subgroups: $n = 3$; 1 high-influence subgroup: $n = 7$; 2 high-influence subgroups:

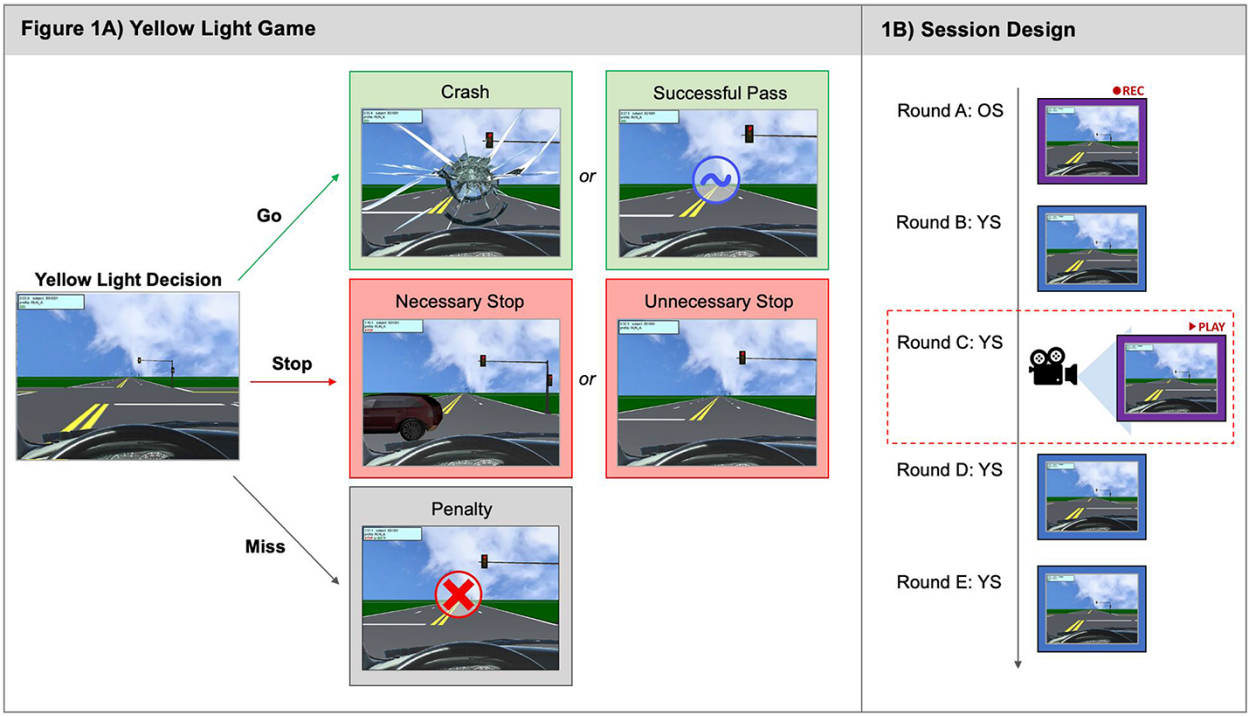

Fig. 1. OS = older sibling; YS = younger sibling. (A) Decision outcomes of YLG. (B) Sequence of YLG rounds across OS (purple outline) and YS (blue outline) sessions. Red box highlights the social learning run of interest.

$n = 11$; 3 high-influence subgroups: $n = 11$; 4 high-influence subgroups: $n = 9$; 5 high-influence subgroups: $n = 3$).

Sibling age spacing

Age spacing between siblings was computed by subtracting adolescent age from older sibling age, with higher scores indicating greater distance in age spacing. Given that the average age spacing between siblings was 2.5 years apart (s.d. = 0.83, min = 1.19, max = 4.28), dyads that were less than 2.5 years apart in age were designated as high influence, whereas those that were more than 2.5 years apart were labeled as low influence. These age subgroups are developmentally appropriate as adolescent siblings closer in age report higher levels of interaction, including intimacy and conflict (Campione-Barr and Killoren, 2019). Separating individuals based on the varied dimensions below allowed for greater insight into the potential brain mechanisms that associate with each type of social learning influence.

Sex composition of sibling dyad

Participants reported on their biological sex, and sibling dyads were separated as same-sex and mixed-sex (i.e. male and female). Same-sex sibling dyads were specified as high influence, whereas mixed-sex dyads were designated as low influence. One participant was excluded due to their recent identification as a transgender individual ($n = 43$).

Adolescent perception of older sibling modeling

Adolescents completed eight items on modeling from the Sibling Influence Scale (Whiteman *et al.*, 2010) to measure the degree to which adolescents perceive that they model their older sibling's behavior. The scale ranged from 1 = *never* to 5 = *very often* with higher scores indicative of higher older sibling influence on adolescent behavior. Two example items included 'From watching my sibling, I have learned how to do things' and 'My sibling gives me advice on how to behave'. The internal reliability was satisfactory (0.733). Adolescents were separated into subgroups based on the scale 3 = *sometimes* such that adolescents who reported more frequent sibling modeling (score ≥ 3) were specified as high influence, whereas adolescents who reported less (score < 3) were designated as low influence. These two subgroups also closely corresponded to a mean split of the data ($M = 2.84$, s.d. = 0.66, min = 1.63, max = 4.38). Four participants were excluded due to missing data ($n = 40$).

Adolescent differentiation from older sibling

Adolescents also completed 10 items from the Sibling Influence Scale (Whiteman *et al.*, 2010) on differentiation or the degree to which they try to act different than their sibling. The scale ranged from 1 = *never* to 5 = *very often* and was reverse coded such that higher scores indicated lower levels of adolescents trying to differentiate from their older siblings. Two example items included 'I live my life differently so I won't be like my sibling' and 'I try to make different choices than my sibling'. The internal reliability was good (0.815). Again, adolescents were separated into subgroups based on the scale 3 = *sometimes* such that adolescents who reported less differentiation from their older sibling (score ≥ 3) were specified as high influence, whereas adolescents who reported more (score < 3) were designated as low influence. These two subgroups also closely corresponded to a mean split of the data ($M = 3.07$, s.d. = 0.69, min = 1.30, max = 4.20). Four participants were excluded due to missing data ($n = 40$).

Adolescent behavior change

Adolescents were separated into subgroups based on their change in behavior between baseline (i.e. first round of the task) and

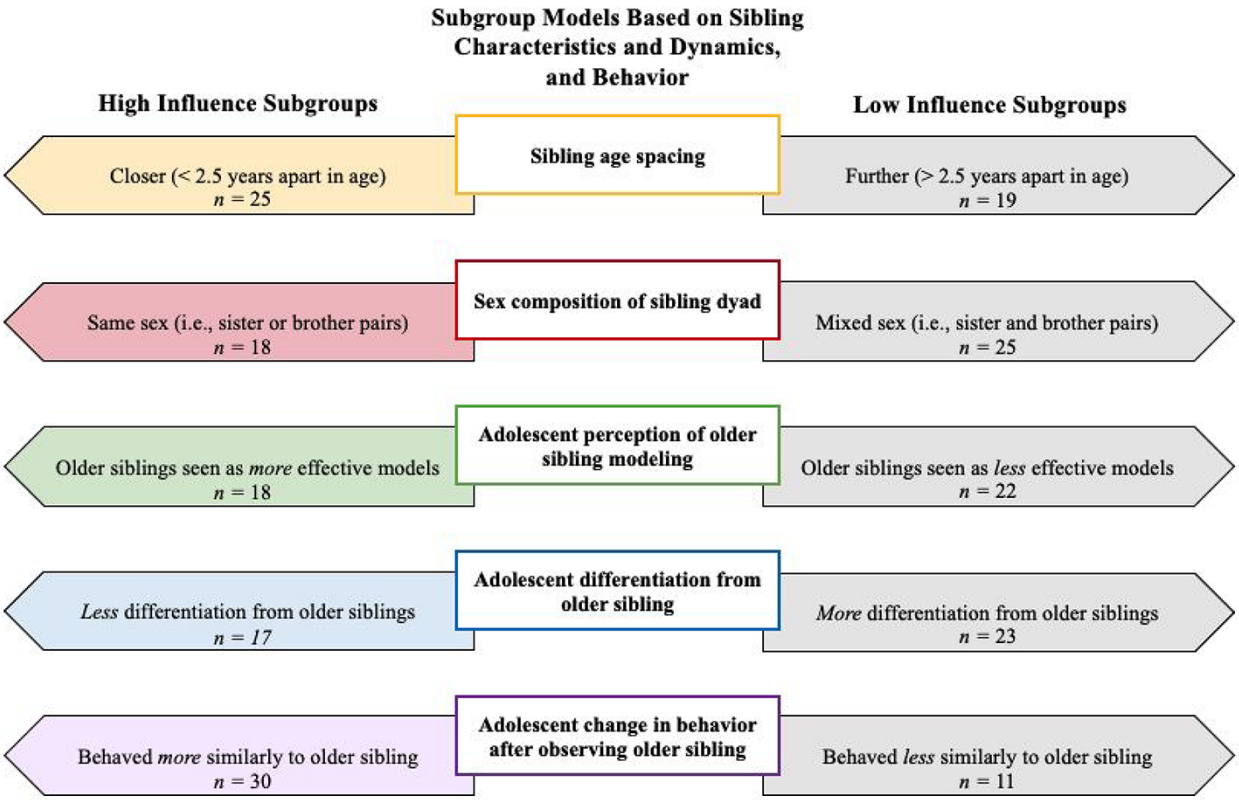

Fig. 2. Five subgroup models were estimated based on high- and low-influence subgroups. Samples sizes for each subgroup are noted in their respective boxes.

after observing their sibling on the YLG. A continuous measure of younger sibling's change in risky behavior toward their older sibling's risky behavior was used from Rogers *et al.* (2021), with positive scores reflecting change toward their sibling, zero reflecting no change and negative scores reflecting change away from their sibling ($M = 2.30$, s.d. $= 3.82$, min $= -7$, max $= 12$). As previously reported, shifts in adolescent behavior were significant such that adolescents changed their behavior toward the behavior of their older sibling following observation (Rogers *et al.*, 2021). These changes in behavior were toward more or less risky behavior, ultimately reflecting the behavior of the older sibling. Subgroups were created based on this variable such that adolescents whose risky behavior changed in the direction of their older sibling's risky behavior were designated as high influence, whereas adolescents whose risky behavior did not change in the direction of their older sibling's risky behavior were specified as low influence, including adolescents who did not change their behavior at all. Three participants were excluded because their baseline rate of risk taking was the same as their older sibling and, thus, change toward similarity could not be examined ($n = 41$).

fMRI data acquisition

Brain images were collected using a research-dedicated 3 Tesla Siemens Prisma MRI scanner. The YLG was presented on a computer screen and projected through a mirror. A high-resolution structural T2*-weighted echo-planar imaging (EPI) volume (repetition time (TR) = 2000 ms; echo time (TE) = 25 ms; matrix = 92 × 92; field-of-view (FOV) = 230 mm; 37 slices; slice thickness = 3 mm;

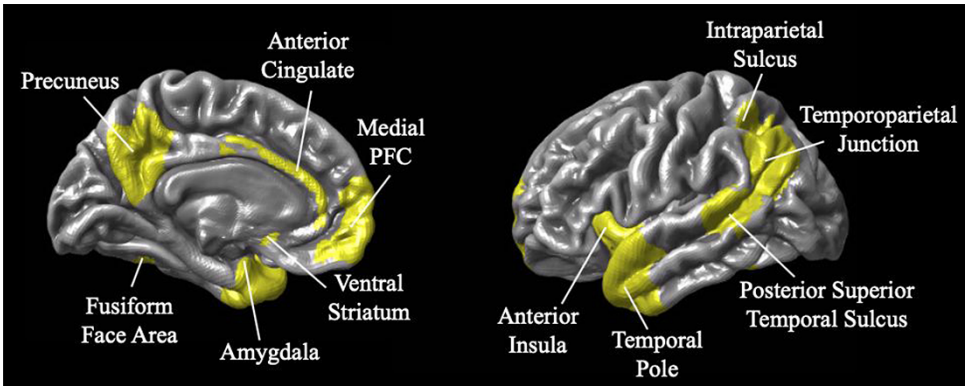

Fig. 3. ROIs used in the fMRI analyses.

voxel size 2.5 × 2.5 × 3 mm^3) was acquired coplanar with a T2*-weighted structural matched-bandwidth (MBW), high-resolution, anatomical scan (TR = 5700 ms; TE = 65 ms; matrix = 192 × 192; FOV = 230 mm; 38 slices; slice thickness = 3 mm). In addition, a T1* magnetization-prepared rapid-acquisition gradient echo (MPRAGE; TR = 2400 ms; TE = 2.22 ms; matrix = 256 × 256; FOV = 256 mm; sagittal plane; slice thickness = 0.8 mm; 208 slices) was acquired. The orientation for the EPI and MBW scans was oblique axial to maximize brain coverage and to reduce noise.

fMRI data preprocessing and analysis

Preprocessing was carried out using FSL (FMRIB's Software Library, version 5.0.10; www.fmrib.ox.ac.uk/fsl). Preprocessing was applied for motion correction using MCFLIRT (Jenkinson *et al.*, 2002), skull stripping using BET (Smith., 2002), spatial smoothing using a 6-mm Gaussian kernel of full width at half maximum, high-pass temporal filtering with a 1280-s cutoff to remove low-frequency drift and grand-mean intensity normalization of the entire 4D dataset by a single multiplicative factor. In addition, independent components analysis (ICA) denoising for motion and physiological noise was conducted using MELODIC (version 3.15) in conjunction with an automated component classifier (Tohka *et al.*, 2008; Neyman–Pearson threshold = 0.3). For spatial normalization, the EPI time series was registered to the T1 image with a linear transformation, followed by a white-matter boundary-based transformation (Greve and Fischl, 2009) using FLIRT. Next, linear and nonlinear transformations to standard Montreal Neurological Institute (MNI) 2-mm brain were performed using Advanced Neuroimaging Tools (ANTs; Avants *et al.*, 2011) and then spatial normalization from the EPI image to MNI space. Participants exhibited motion of less than 2 mm for inter-slice movement on 90% or more of slices; however, slices with greater than 3 mm of motion were scrubbed from each individual's time series to eliminate spikes in movement across each time series. After scrubbing, the time-series data ranged from 93 to 114 TRs ($M = 104.23$; s.d. = 5.12).

A time series of each a priori region of interest (ROI) was extracted for each participant. A total of 20 a priori ROIs were selected based on previous neuroimaging work examining the social brain and risk taking during adolescence (McCormick *et al.*, 2018; van Hoorn *et al.*, 2019). ROIs included the left and right VS given their relation to reward processing during risk taking (Schreuders *et al.*, 2018), as well as the salience of reward processing in social contexts during adolescence (Telzer *et al.*, 2018; van Hoorn *et al.*, 2019), and were defined via Neurosynth by searching 'ventral striatum' and thresholding the resulting meta-analytic image at $Z = 14$. In addition, 18 brain regions were identified as salient in functional connectivity of the social brain during adolescence and defined based on the ROIs used in McCormick *et al.* (2018), including bilateral masks of the AI, temporal poles (TP), posterior STS (pSTS), IPS, TPJ, amygdala, mPFC and FFA, as well as the ACC and precuneus. These ROIs were defined from a number of sources, including the Harvard-Oxford (ACC, AI, amygdala; Harvard Center for Morphometric Analysis) and SPM Anatomy toolbox (IPS, TP, FFA; Eickhoff *et al.*, 2005) probabilistic atlases, the Saxe Lab social brain ROIs (TPJ, precuneus; Dufour *et al.*, 2013) and the social brain ROIs defined by (Blakemore and Mills, 2014). (mPFC, pSTS). No ROIs had any overlapping voxels. A brain map containing all the ROI masks is shown in Figure 3 and is available on Neurovault (https://neurovault.org/collections/GCIXDBNW/).

Group iterative multiple model estimation

The time series from the entire social learning run (i.e. adolescents' observation of their older sibling's performance on the YLG), including decisions and feedback trials, was used in GIMME (Gates and Molenaar, 2012). GIMME utilizes heterogeneous individual- and group-level information to reliably examine patterns of directional brain region connectivity and construct functional. Although each participant's time series was a different length due to the self-paced nature of the YLG, GIMME can model unequal amounts of data between participants (Gates *et al.*, 2014). And while prior work has shown that improvement in recovery of paths occurs as the length of time increases, we had more than adequate lengths of time for all participants (far greater than the $T = 60$ minimum suggested by prior simulation work; Lane *et al.*, 2019). Additionally, prior work has confirmed that GIMME performs well in identifying subgroup-specific paths even when the subgroup sizes are unequal and has been tested for use with sample or subgroup sizes as low as 7 per subgroup (Gates *et al.*, 2017). Furthermore, GIMME performs satisfactorily modeling up to 20 ROIs (Henry *et al.*, 2019).

GIMME provides estimates for contemporaneous (cross-sectional effects between ROIs; i.e. ROI_1 at t predicts ROI_2 at t), lagged (longitudinal effects between ROIs; i.e. ROI_1 at t-1 predicts ROI_2 at t) and autoregressive (longitudinal effects within ROIs) pathways in the same analytic model. Importantly, including the autoregressive effects improves the accuracy in recovering the true directionality of the paths (Lane and Gates, 2017). Group-level paths must yield significance ($P < 0.001$) for at least 75% of individuals to qualify as a group path, and all other individual paths are kept if they improve model fit. Thus, significant pathways for the majority of individuals are estimated, whereas pathways that are nonsignificant are set to zero across individuals, yielding a group-level map that represents the majority of the sample, as well as individual-level paths (Henry *et al.*, 2019). Of note, GIMME corrects for multiple comparisons at $P < 0.05$ per the number of paths tested per person and the number of subjects. Further, GIMME encompasses a parsimonious approach as it stops model-building once the model obtains a good fit, which together yields to a very low false-positive rate (Nestler and Humberg, 2021). GIMME is freely available through the open-source R platform, and additional model information can be found in Gates *et al.* (2017).

Subgroup-level analyses on predefined subsets of individuals can also be performed using GIMME in an extension called confirmatory subgroup GIMME (CS-GIMME), which can also

Table 2. Differences in younger sibling risky behavior toward older sibling risky behavior by high- and low-influence subgroups

	Difference in behavior toward older sibling		
Subgroup models	**High influence M (s.d.)**	**Low influence M (s.d.)**	***t*-value**
Sibling age spacing	3.40 (3.61)	0.74 (3.57)	2.437*
Sex composition	2.42 (3.44)	2.12 (4.11)	0.258
Older sibling modeling	2.96 (3.00)	1.22 (4.61)	1.519
Adolescent differentiation	2.90 (3.96)	1.65 (3.61)	1.092

Note: M = mean; s.d. = standard deviation. Risky behavior measured as number of go decisions younger adolescents took in the Yellow Light Game.
*$P < 0.05$. Two-tailed significance.

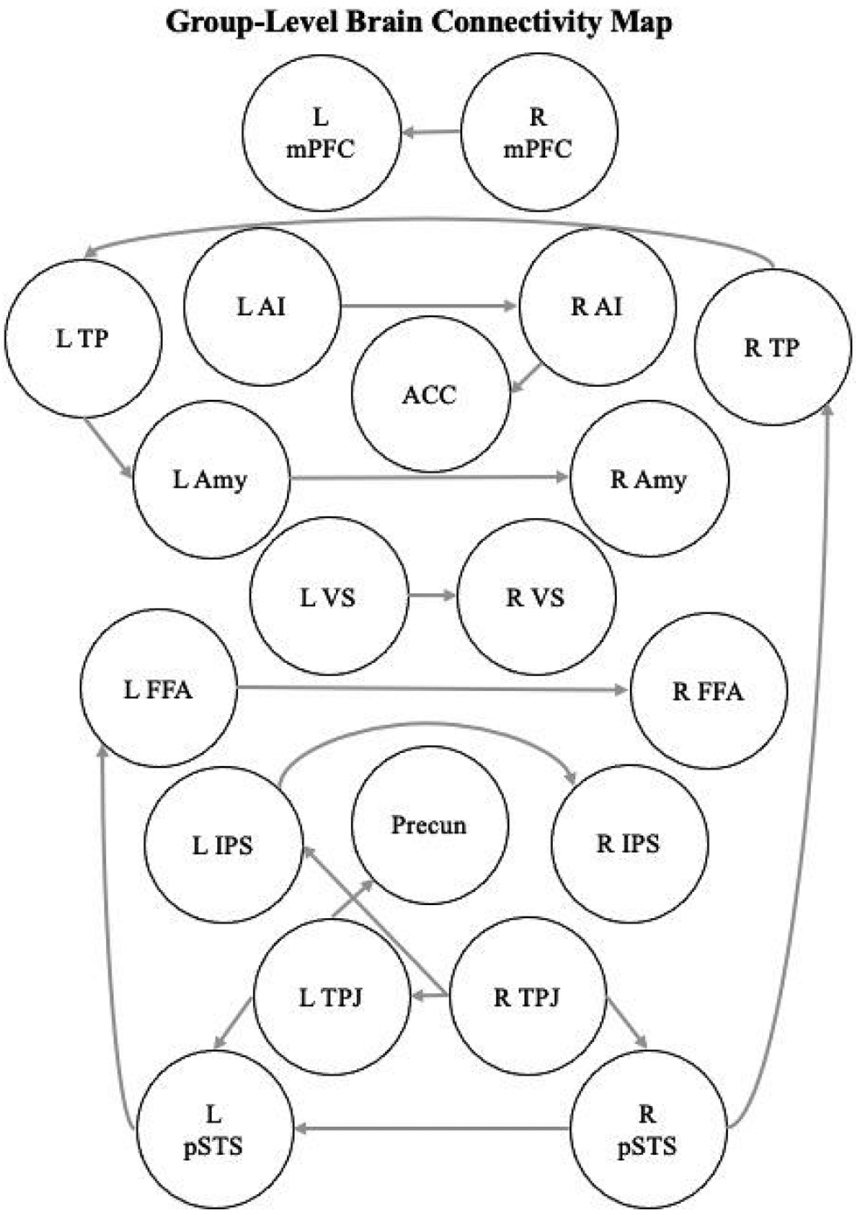

Fig. 4. Group-level brain connectivity map showing directional pathways for at least 75% of focal adolescents during observation of older sibling decision-making.

L = left; R = right; mPFC = medial prefrontal cortex; TP = temporal pole; AI = anterior insula; ACC = anterior cingulate cortex; Amy = Amygdala; VS = ventral striatum; FFA = fusiform face area; IPS = intraparietal sulcus; Precun = Precuneus; TPJ = temporal parietal junction; pSTS = posterior superior temporal sulcus. Autoregressive paths (brain region predicted by same brain region previously) were estimated but not shown in the figure. All brain region paths were contemporaneous associations.

satisfactorily model up to 20 ROIs (Henry *et al.*, 2019). This approach uses a priori subgroup assignments to examine additional paths that emerge for each respective subgroup. Significant subgroup pathways will yield a beta coefficient and undergo Bonferoni correction at $P < 0.05$, *whereas* nonsignificant pathways across individuals are constrained to zero. Five sets of CS-GIMME results were examined to identify adolescents who may be highly susceptible versus less susceptible to social influence based on social learning theory and behavioral findings. These subgroup models included: sibling age spacing, sex constellation of the sibling dyad, older sibling modeling, adolescent differentiation from older siblings and adolescent behavioral change toward older sibling behavior (see Figure 2). The lowest sample size for a subgroup included 11 participants, which is satisfactory for CS-GIMME to perform well (Henry *et al.*, 2019).

Results

Group-level results

We first examined the group-level connectivity patterns in the adolescent brain during the observation of older sibling risk taking. These group-level paths existed across all five of the subgroup allocation analyses, suggesting that these paths consistently exist for adolescents engaged in this task. Group paths included associations between all nine bilateral brain regions, which are displayed in Table 3 and Figure 4. Paths appeared from the AI to the

ACC and from the TP to the amygdala. Paths from the bilateral TPJ to the bilateral pSTS also emerged, with paths from the pSTS to the TP and FFA. In addition, the TPJ also exhibited a path to the precuneus and the IPS.

Subgroup-level results

Behavioral differences

We first conducted analyses to determine whether the high- and low-influence subgroups showed significant changes in behavior presocial and postsocial learning. Independent samples *t*-tests were conducted to compare high- and low-influence subgroups, with the exception of the subgroup for adolescent change in behavior to avoid redundancy (Table 2). Specifically, these tests examined differences in the degree to which younger sibling risky behaviors changed in the direction of their older sibling's risky behaviors (using the continuous measure of behavior change, as described in the methods section) between high- and low-influence subgroups. Significant differences in behavior emerged for the sibling age spacing subgroups such that adolescents in the high-influence subgroup (i.e. closer in age to sibling) showed more change in behavior toward their older sibling than the low-influence subgroup (i.e. further in age to sibling; $t(42) = 2.44$, $P = 0.019$, 95% CI [0.457, 4.869], $d = 0.742$). The other three subgroup models did not exhibit significant differences in behavior from baseline to after observing older sibling performance. Of note, these three subgroups did yield the expected patterns of behavioral differences as adolescents in high-influence subgroups tended to exhibit a higher change in behavior compared low-influence subgroups (see Table 2).

Subgroup-level connectivity

Subgroup-level connectivity analyses were conducted based on social learning influence factors including dyad sex, age spacing, modeling, differentiation and behavior (Figure 2). Each of these subgroup models included a high-influence subgroup and a low-influence subgroup, which are displayed in Supplemental Figures S1–S5. In addition, collective patterns for high-influence subgroups and low-influence subgroups are reported.

Table 3. Group-level connectivity pathways (supplement to Figure 4)

Paths	β	s.d.
R mPFC → L mPFC	0.61	0.15
L AI → R AI	0.69	0.13
L TPJ → Precun	0.45	0.17
L IPS → R IPS	0.61	0.20
R TPJ → R pSTS	0.52	0.35
R pSTS → L pSTS	0.45	0.25
R TPJ → L TPJ	0.52	0.24
L FFA → R FFA	0.50	0.17
R TP → L TP	0.60	0.21
L Amy → R Amy	0.51	0.20
L VS → R VS	0.56	0.18
L pSTS → L FFA	0.38	0.19
L TP → L Amy	0.45	0.21
L TPJ → L pSTS	0.42	0.21
R pSTS → R TP	0.35	0.22
R TPJ → L IPS	0.34	0.34
R AI → ACC	0.37	0.21

Note: Significant group-level contemporaneous pathways. No lagged pathways were significant.
L = left; R = right; mPFC = medial prefrontal cortex; TP = temporal pole; AI = anterior insula; ACC = anterior cingulate cortex; Amy = Amygdala; VS = ventral striatum; FFA = fusiform face area; IPS = intraparietal sulcus; Precun = Precuneus; TPJ = temporal parietal junction; pSTS = posterior superior temporal sulcus.

Table 4. High-influence subgroup-level pathways (supplement to Figure 5)

Paths	β	s.d.
Closer in age		
L TPJ → L mPFC	0.33	0.22
R pSTS → R FFA	0.22	0.19
R pSTS → R AI	0.15	0.28
L Amy → L AI	0.43	0.26
R TPJ → R mPFC	0.25	0.24
L TP → R mPFC	0.17	0.19
Same sex		
R AI → R TPJ	0.28	0.24
R AI → R TP	0.31	0.15
R AI → R mPFC	0.17	0.19
L TPJ → R mPFC	0.28	0.20
More effective model		
R FFA → Precun	0.10	0.18
L Amy → L AI	0.35	0.25
Lag: R TPJ → L TPJ	−0.30	0.17
Less differentiation		
R TPJ → Precun	0.33	0.11
ACC → L VS	0.36	0.17
R AI → R TPJ	0.23	0.19
R VS → R mPFC	0.15	0.14
L TPJ → R mPFC	0.22	0.24
R mPFC → R TP	0.22	.30
Lag: R TPJ → L pSTS	−0.18	0.14
Lag: R IPS → L mPFC	−0.07	0.11
More similar behavior		
R TPJ → Precun	0.30	0.17
R mPFC → ACC	0.21	0.18
R TP → R Amy	0.30	0.25
R pSTS → R FFA	0.21	0.19
Lag: L IPS → R IPS	−0.29	0.19

Note: Significant subgroup-level pathways for high-influence adolescents during observation of older sibling decision-making. Lagged pathways are denoted with '*Lag*'. All others represent contemporaneous associations.
L = left; R = right; mPFC = medial prefrontal cortex; TP = temporal pole; AI = anterior insula; ACC = anterior cingulate cortex; Amy = Amygdala; VS = ventral striatum; FFA = fusiform face area; IPS = intraparietal sulcus; Precun = Precuneus; TPJ = temporal parietal junction; pSTS = posterior superior temporal sulcus.

Neural paths in high-influence subgroups. Paths for the high-influence subgroups are displayed in Table 4 and Figure 5. Several collective patterns are noted. First, the AI and mPFC served as hubs for connectivity across most of the subgroups. The AI evidenced input from the pSTS and the amygdala, and output to the mPFC, TPJ and TP. Further, the mPFC exhibited input from several regions (e.g. TPJ, TP, AI and VS) and displayed output to the TP and ACC. Second, subcortical regions, such as the amygdala and VS, provided input to the AI and mPFC, whereas the AI and mPFC did not provide input to subcortical regions. The direction of pathways from subcortical structures to cortical structures suggests bottom-up processes. Third, several subgroups evidenced significant lagged pathways that were negative, such that higher activation in one brain region predicted later lower activation in a different brain region across the task. The TPJ and IPS evidenced these lagged negative pathways to the pSTS, mPFC and the corresponding hemispheric region.

Neural paths in low-influence subgroups. Paths for the low-influence subgroups are displayed in Table 5 and Figure 6. Several

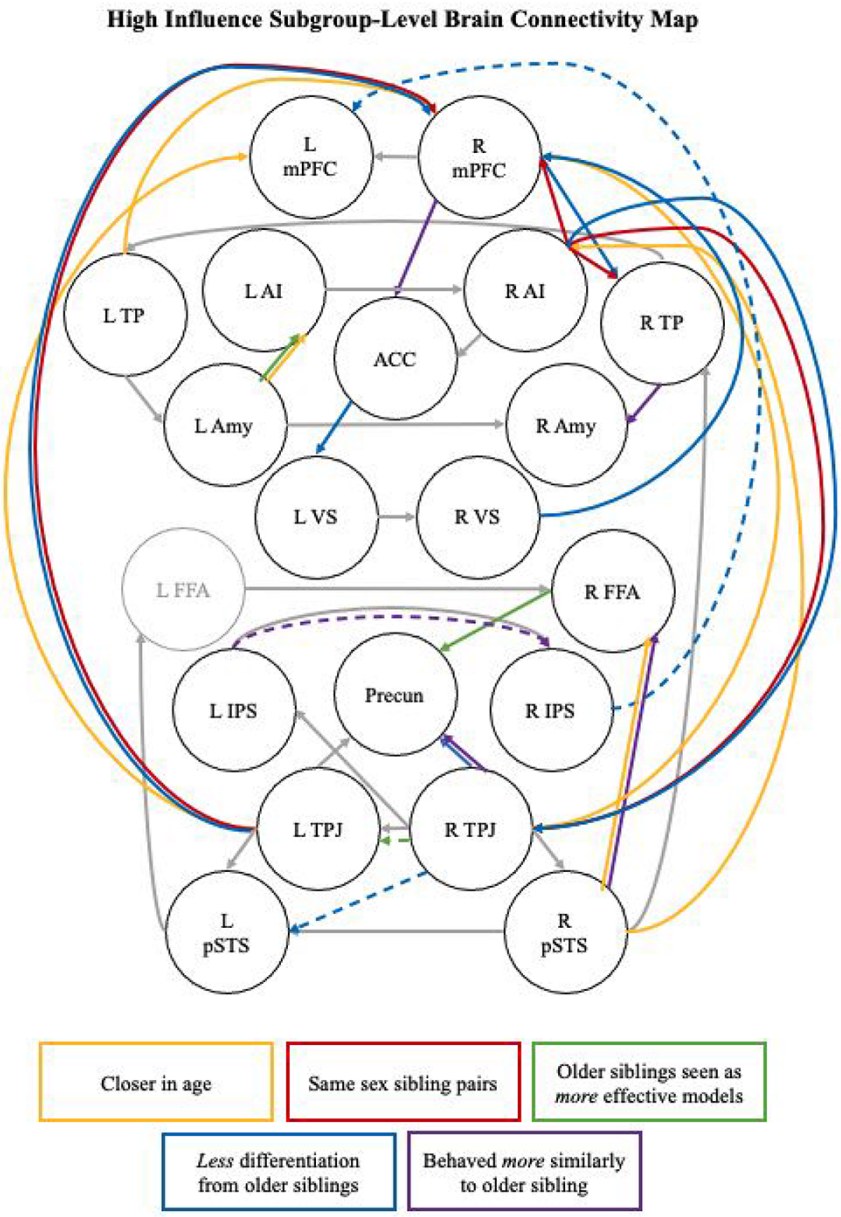

Fig. 5. Subgroup-level brain connectivity map showing directional pathways for high-influence adolescents during observation of older sibling decision-making.

L = left; R = right; mPFC = medial prefrontal cortex; TP = temporal pole; AI = anterior insula; ACC = anterior cingulate cortex; Amy = Amygdala; VS = ventral striatum; FFA = fusiform face area; IPS = intraparietal sulcus; Precun = Precuneus; TPJ = temporal parietal junction; pSTS = posterior superior temporal sulcus. Subgroup-level connectivity map showing directional pathways. Arrow colors indicate pathways for high-influence subgroups compared to low-influence subgroups, where grey reflects group-level pathways. Autoregressive paths (brain region predicted by same brain region previously) were estimated but not shown in the figure. Solid arrow paths represent maps contemporaneous associations, whereas dashed arrow paths represent lagged paths across observation.

collective patterns are observed. First, consistent with the high-influence subgroups, low-influence subgroups showed a pattern of concentrated pathways to and from the mPFC as a hub of connectivity, exhibited by input from the TPJ and TP and output to the TPJ, TP, VS and ACC. In kind, the AI emerged as a region that provided substantial output to other brain regions, including the TPJ, TP, FFA, pSTS and amygdala. However, this region did not exhibit input from other brain regions. Second, in contrast with high-influence subgroups, subcortical regions, such as the amygdala and VS, received input from the AI and mPFC. However, the opposite direction of pathways was not exhibited. The direction of pathways from subcortical structures to cortical structures suggests top-down processes. Third, two low-influence subgroups evidenced significant lagged pathways that were negative. Although these pathways were half in number compared to the high-influence subgroups, the TPJ and precuneus provided lagged negative input to the TPJ and IPS.

Discussion

Although social learning theory provides a framework for examining how adolescents adopt and internalize social norms through

observation (Bandura, 1977), it is advantageous to better understand the neural mechanisms that underlie this process. Developmental neuroscience has identified potential neural candidates that may underlie social learning processes, including the neural correlates of adolescent decision-making in social contexts (for a meta-analysis, see van Hoorn *et al.*, 2019), but these methods typically do not account for within-individual and within-group variability which is important for capturing individual differences. In addition, prior work heavily relies on analyses that test univariate brain activation rather than connectivity across key brain regions. Thus, we used a social learning paradigm with older siblings and an analysis that incorporated both individual and group differences (i.e. GIMME). We identified group-level pathways underlying social observation in the adolescent brain, as well as pathways specific to adolescents who were more, or less, likely to engage in social learning. These findings highlight collective patterns of how adolescents process information in the brain during social observation, as well as important pathways in the brain that are model-dependent based on factors associated with social learning theory.

Two neural mechanisms of social observation appeared across adolescents. First, the pathway from the AI to the ACC emerged as an important pathway for adolescents to process information during social learning, consistent with a recent paper exploring risky decision-making using GIMME (McCormick *et al.*, 2019). The insular cortex serves as a hub and guides the salience network in determining which aspects of the environment are salient to attend to, specifically through coordination with the ACC to drive other networks, such as the central external network to initiate actions (Uddin, 2015). Dynamic functional connectivity within this network occurs when individuals attend to environments with fluctuating stimuli (Kucyi *et al.*, 2017), highlighting the importance of the salience network in learning in complex environments, particularly ones with social models. Our finding suggests that the pathway from the AI to the ACC may be foundational in processing information during social observation of risky decision-making. Second, we found that mentalizing regions involved in perspective-taking and identifying relevant social information, including the TPJ and TP (Blakemore and Mills, 2014; Welborn *et al.*, 2016; Lin *et al.*, 2018), provided input to social cognition regions, such as the pSTS, FFA and precuneus, which specifically encode, identify salience and track errors in social information (Gunther Moor *et al.*, 2012; Zerubavel *et al.*, 2015; Stephanou *et al.*, 2016). These pathways may facilitate the identification of the utility of observing and integrating information from a specific social context across adolescents. Together these findings suggest that salience detection, via the AI to the ACC pathway, and mentalizing, via a social cognition pathway including the TP and TPJ to the pSTS, FFA and precuneus, are important neural mechanisms of observation during adolescent social learning.

Interestingly, the AI and mPFC both served as connectivity hubs to provide contextual social information during social observation, but their roles were dependent on the influential nature of the older sibling on adolescent social learning. For younger siblings who are more likely to be influenced by their older siblings, we found that affective regions such as the VS and amygdala directed functional connectivity to the AI, a brain region associated with salience detection and decision-making (Smith *et al.*, 2014; Uddin, 2015), and the mPFC, a brain region implicated in regulation and value-based decision-making (McCormick and Telzer, 2017; Blankenstein *et al.*, 2018), during social observation. This trend of affective brain regions driving decision-making regions may reflect that adolescents who are highly influenced by a given social model use affective information to inform the salience of information and their decisions to incorporate and update their schema of risky decision-making during social learning. On the other hand, for younger siblings who are less likely to be influenced by their older siblings, the AI and mPFC provided contextual social information to affective regions, including the VS and amygdala, to inform social learning. These findings align with prior research, such that the mPFC directed connectivity to the amygdala during risky decision-making for adolescents, compared to adults (McCormick *et al.*, 2019). Functional connectivity from the mPFC to the amygdala has been proposed as a neurobiological mechanism underlying downregulation, a critical process in guiding behavior in socioemotional contexts, particularly during adolescence (Hare *et al.*, 2008). Given that less salient social models elicited downregulation connectivity when adolescents engaged in social observation

Table 5. Low-influence subgroup-level pathways (supplement to Figure 6)

Paths	B	s.d.
Further in Age		
R FFA → Precun	0.19	0.13
R AI → R TPJ	0.24	0.24
R AI → R TP	0.30	0.20
R TP → R mPFC	0.24	0.25
L TP → L mPFC	0.15	0.12
R TP → R FFA	0.17	0.15
L mPFC → L TPJ	0.25	0.21
L AI → L Amy	0.25	0.23
L AI → L TP	0.28	0.14
Lag: Precun → L IPS	–0.27	0.19
Mixed sex		
L TP → R mPFC	0.19	0.17
R TPJ → R mPFC	0.27	0.21
Lag: R TPJ → L TPJ	–0.29	0.16
Less effective model		
L TP → L AI	0.34	0.21
ACC → R TPJ	0.25	0.29
L mPFC → R TP	0.26	0.21
R TPJ → L mPFC	–0.22	0.16
L AI → L Amy	0.38	0.26
More differentiation		
R mPFC → L VS	0.19	0.21
R FFA → Precun	0.15	0.10
R pSTS → R FFA	0.25	0.21
L TP → R mPFC	0.13	0.17
R TPJ → R mPFC	0.28	0.22
Less similar behavior		
R AI → R Amy	0.37	0.27
L mPFC → ACC	0.34	0.14
R Amy → R TP	0.25	0.25
R TP → R mPFC	0.27	0.23
R AI → R TPJ	0.23	0.13
R FFA → Precun	0.15	0.13
R AI → R pSTS	0.18	0.13
R AI → R FFA	0.14	0.15

Note: Significant subgroup-level pathways for low-influence adolescents during observation of older sibling decision-making. Lagged pathways are denoted with '*Lag*'. All others represent contemporaneous associations. L = left; R = right; mPFC = medial prefrontal cortex; TP = temporal pole; AI = anterior insula; ACC = anterior cingulate cortex; Amy = Amygdala; VS = ventral striatum; FFA = fusiform face area; IPS = intraparietal sulcus; Precun = Precuneus; TPJ = temporal parietal junction; pSTS = posterior superior temporal sulcus.

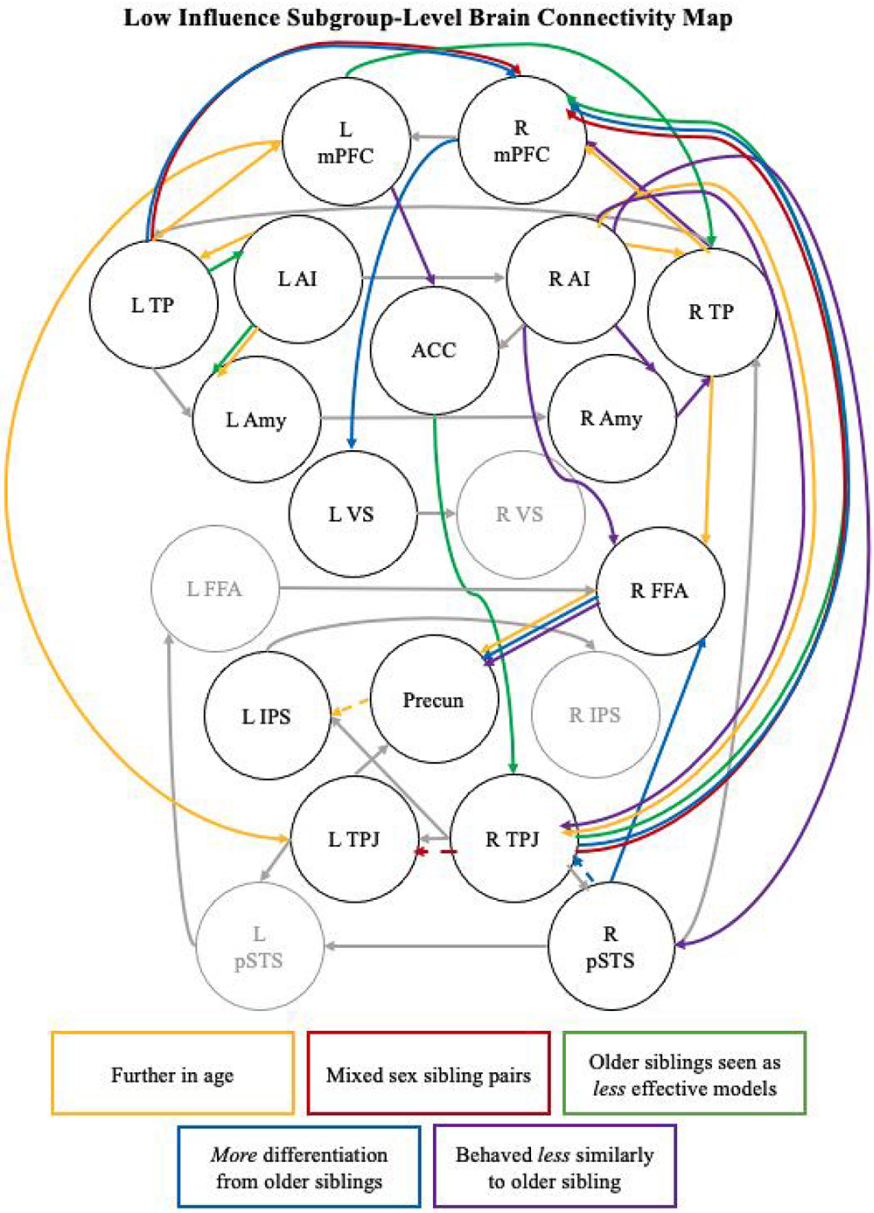

Fig. 6. Subgroup-level brain connectivity map showing directional pathways for low-influence adolescents during observation of older sibling decision-making.

L = left; R = right; mPFC = medial prefrontal cortex; TP = temporal pole; AI = anterior insula; ACC = anterior cingulate cortex; Amy = Amygdala; VS = ventral striatum; FFA = fusiform face area; IPS = intraparietal sulcus; Precun = Precuneus; TPJ = temporal parietal junction; pSTS = posterior superior temporal sulcus. Subgroup-level connectivity map showing directional pathways. Arrow colors indicate pathways for low-influence subgroups compared to high-influence subgroups, where grey reflects group-level pathways. Autoregressive paths (brain region predicted by same brain region previously) were estimated but not shown in the figure. Solid arrow paths represent maps contemporaneous associations, whereas dashed arrow paths represent lagged paths across observation.

in this study, this neurobiological mechanism may enable adolescents to resist social influence and more efficiently evaluate the salience of the observed behavior (Morawetz *et al.*, 2017). Interestingly, this finding contrasts with neural connectivity of high-influence adolescents, such that more salient social models elicited upregulation connectivity, which likely underlies learning that is more highly motivated by the rewarding nature of social cues. Together, these findings suggest that the influential nature of social models engender opposing trends in the neurobiological mechanisms that underlie adolescent social observation of risk behavior.

In addition to neural connectivity trends across adolescents in high- and low-influence subgroups, there were many unique pathways that emerged depending on factors associated with social learning theory, including age spacing, sex constellation, modeling, differentiation and real-world behavior in relation to their older sibling as a social model. These unique pathways provide a starting point to better understand how different aspects of the relationship between a learner and social model can inform the underlying neural mechanisms of social learning. Specifically, similarity (or dissimilarity) in characteristics, such as age spacing and sex constellation, elicited different neural connectivity compared to the attitudes about the social model, including modeling and differentiation, and compared to the learner's change in behavior toward (or away from) the social model. Given that similarity, attitudes and behavior each elicit different patterns

in neural connectivity during social learning, which likely underlies differences in information processing, this study highlights the importance of considering a breadth of factors that may contribute to whether learners are motivated to learn from specific social models. Of note, the only instance of negative contemporaneous functional connectivity occurred from the TPJ to the mPFC for adolescents who perceived their older siblings as less salient models compared to adolescents who perceived more salient modeling. This finding suggests that greater activation in the TPJ, a region associated with mentalizing and identifying salient social cues, may simultaneously downregulate activation in the mPFC, a brain region associated with social decision-making, for adolescents who are not easily influenced in a given context. Although some literature indicates that affective regions, such as the amygdala and VS, may downregulate the mPFC while youth make decisions in the context of salient social agents, such as mothers (Gee *et al.*, 2014; Guassi Moreira and Telzer, 2018; Rogers *et al.*, 2020), this work provides preliminary evidence that social cognition brain regions may play a role in downregulation in less influential contexts. Together, these findings have clear implications for the significance of variability between adolescents who learn from a social model, as well as variability within these groups based on social learning factors.

To our knowledge, this is the first study to examine directional neural connectivity patterns underlying adolescent social observation using group-, subgroup- and individual-level variability. Although it provides an initial foundation for future directions, the limitations of this study should be noted. First, 20 ROIs were chosen for this study based on recent seminal papers that rigorously examined brain regions associated with adolescent decision-making in social contexts (i.e. McCormick *et al.*, 2019; van Hoorn *et al.*, 2019), but selecting different ROIs would likely lead to a different set of findings. Relatedly, GIMME and CS-GIMME do not model analyses across the entire brain and, as such, require careful consideration of ROI inclusion (Henry *et al.*, 2019). Second, because sibling behavior can be a salient predictor of adolescent attitudes, learning and behavior (for a review, McHale *et al.*, 2012), this study used dyads of adolescent siblings to examine directional functional connectivity in the brain during a social learning paradigm. Future work would benefit from investigating whether the findings in this study are specific to older sibling models or whether social learning from individuals with a shared history (e.g. parents, younger siblings, best friends and teachers) prompt similar patterns of directed neural connectivity. In kind, the real behavior of older siblings was used for the observation phase to provide ecological validity to the social learning paradigm; however, this decision limited our ability to test for controlled differences between risky and cautious social models. Third, although this study used dyadic characteristics at multiple levels to examine connectivity maps of social observation, the individual characteristics of adolescents were not investigated. It would be beneficial for future work to focus on age, pubertal status and gender to explore whether directional functional connectivity during social learning varies as a function of these individual differences. Last, given that the majority of the sibling dyads were full biological siblings, future work should replicate this study using genetically informed designs to examine the extent to which shared genetics and environment contribute to the neural mechanisms underlying social learning.

In conclusion, the current study provides a basis for investigating adolescent neural states during social learning. The use of an innovative social learning paradigm, and rigorous analyses that utilize both individual and group heterogeneity, allowed us to identify directional neural connectivity during social observation across adolescents and between subgroups of adolescents based on tenets of social learning theory. We found that adolescents neurobiologically responded to information differentially depending on the salience of models, highlighting the importance of teens being able to, and wanting to, identify with social learning models. These findings direct future work to better understand how different levels of model influence associate with different connectivity networks and which of these networks may represent 'mature' social information processing to promote adolescent learning.

Acknowledgements

We greatly appreciate Elise Breitfeld, Sue Hyun Kwon and Madison Marcus for their diligence in recruitment, data management and data collection. We also thank Amanda Carter Benjamin, Susannah Ivory and Virnaliz Jimenez for their assistance in collecting data.

Funding

This research was supported by the National Institutes of Health (R01DA039923 to E.H.T.) and the National Science Foundation (BCS 1539651 to E.H.T.).

Conflict of interest

The authors declared that they had no conflict of interest with respect to their authorship or the publication of this article.

Supplementary data

Supplementary data is available at *SCAN* online.

Data availability

The data that support the findings of this study are available on request from the corresponding author. The data are not publicly available due to privacy or ethical restrictions.

REFERENCES

Akers, R.L., Krohn, M.D., Lanza-Kaduce, L., Radosevich, M. (1979). Social learning and deviant behavior: a specific test of a general theory. *American Sociological Review*, **44**, 636–55.

Avants, B.B., Tustison, N.J., Song, G., Cook, P.A., Klein, A., Gee, J.C. (2011). A reproducible evaluation of ANTs similarity metric performance in brain image registration. *NeuroImage*, **54**, 2033–44.

Bandura, A. (1977). Self-efficacy: toward a unifying theory of behavioral change. *Psychological Review*, **84**, 191–215.

Blakemore, S.-J., Mills, K.L. (2014). Is adolescence a sensitive period for sociocultural processing? *Annual Review of Psychology*, **65**, 187–207.

Blakemore, S.-J., Robbins, T.W. (2012). Decision-making in the adolescent brain. *Nature Neuroscience*, **15**, 1184–91.

Blankenstein, N.E., Schreuders, E., Peper, J.S., Crone, E.A., van Duijvenvoorde, A.C.K. (2018). Individual differences in risk-taking tendencies modulate the neural processing of risky and ambiguous decision-making in adolescence. *NeuroImage*, **172**, 663–73.

Buchanan, J.P., McGue, M., Keyes, M., Iacono, W.G. (2009). Are there shared environmental influences on adolescent behavior? Evidence from a study of adoptive siblings. *Behavior Genetics*, **39**, 532–40.

Campione-Barr, N., Killoren, S.E. (2019). Love them and hate them: the developmental appropriateness of ambivalence in the adolescent sibling relationship. *Child Development Perspectives*, **13**, 221–6.

Casey, B.J., Heller, A.S., Gee, D.G., Cohen, A.O. (2019). Development of the emotional brain. *Neuroscience Letters*, **693**, 29–34.

Chein, J., Albert, D., O'Brien, L., Uckert, K., Steinberg, L. (2011). Peers increase adolescent risk taking by enhancing activity in the brain's reward circuitry. *Developmental Science*, **14**, F1–10.

Christakis, N.A., Fowler, J.H. (2013). Social contagion theory: examining dynamic social networks and human behavior. *Statistics in Medicine*, **32**, 556–77.

D'Amico, E.J., Fromme, K. (1997). Health risk behaviors of adolescent and young adult siblings. *Health Psychology*, **16**, 426–32.

Duncan, T.E., Duncan, S.C., Hyman, H. (1996). The role of parents and older siblings in predicting adolescent substance use: modeling development via structural equation latent growth methodology. *Journal of Family Psychology*, **10**, 158–72.

Dufour, N., Redcay, E., Young, L., *et al.* (2013). Similar Brain Activation during False Belief Tasks in a Large Sample of Adults with and without Autism. *PLoS One*, **8**(9), e75468.

Eickhoff, S.B., Stephan, K.E., Mohlberg, H., *et al.* (2005). A new SPM toolbox for combining probabilistic cytoarchitectonic maps and functional imaging data. *NeuroImage*, **25**(4), 1325–35.

Ennett, S.T., Bauman, K.E., Hussong, A., *et al.* (2006). The peer context of adolescent substance use: Findings from social network analysis. *Journal of Research on Adolescence*, **16**, 159–86.

Feinberg, M.E., Hetherington, E.M. (2000). Sibling differentiation in adolescence: implications for behavioral genetic theory. *Child Development*, **71**, 1512–24.

Foulkes, L., Leung, J.T., Fuhrmann, D., Knoll, L.J., Blakemore, S.J. (2018). Age differences in the prosocial influence effect. *Developmental Science*, **21**(6), 1–9.

Furman, W., Buhrmester, D. (1985). Children's perceptions of the personal relationships in their social networks. *Developmental Psychology*, **21**(6), 1016–24.

Gardner, M., Steinberg, L. (2005). Peer influence on risk taking, risk preference, and risky decision making in adolescence and adulthood: an experimental study. *Developmental Psychology*, **41**, 625–35.

Gates, K.M., Molenaar, P.C.M., Iyer, S.P., Nigg, J.T., Fair, D.A. (2014). Organizing heterogeneous samples using community detection of GIMME-derived resting state functional networks. *PLoS One*, **9**, 1–11.

Gates, K.M., Lane, S.T., Varangis, E., Giovanello, K., Guiskewicz, K. (2017). Unsupervised classification during time-series model building. *Multivariate Behavioral Research*, **52**, 129–48.

Gates, K.M., Molenaar, P.C.M. (2012). Group search algorithm recovers effective connectivity maps for individuals in homogeneous and heterogeneous samples. *NeuroImage*, **63**, 310–9.

Gee, D.G., Gabard-Durnam, L., Telzer, E.H., *et al.* (2014). Maternal buffering of human amygdala-prefrontal circuitry during childhood but not during adolescence. *Psychological Science*, **25**, 2067–78.

Greve, D.N., Fischl, B. (2009). Accurate and robust brain image alignment using boundary-based registration. *NeuroImage*, **48**, 63–72.

Guassi Moreira, J.F., Telzer, E.H. (2018). Mother still knows best: maternal influence uniquely modulates adolescent reward sensitivity during risk taking. *Developmental Science*, **21**, 1–11.

Gunther Moor, B., Op de Macks, Z.A., Güroğlu, B., Rombouts, S.A.R.B., Van der Molen, M.W., Crone, E.A. (2012). Neurodevelopmental changes of reading the mind in the eyes. *Social Cognitive and Affective Neuroscience*, **7**, 44–52.

Hamilton, A.F.D.C., Grafton, S.T. (2006). Goal representation in human anterior intraparietal sulcus. *Journal of Neuroscience*, **26**, 1133–7.

Hare, T.A., Tottenham, N., Galvan, A., Voss, H.U., Glover, G.H., Casey, B.J. (2008). Biological substrates of emotional reactivity and regulation in adolescence during an emotional go-nogo task. *Biological Psychiatry*, **63**, 927–34.

Henry, T.R., Feczko, E., Cordova, M., *et al.* (2019). Comparing directed functional connectivity between groups with confirmatory subgrouping GIMME. *NeuroImage*, **188**, 642–53.

Jenkinson, M., Bannister, P., Brady, J.M., Smith, S.M. (2002). Improved optimisation for the robust and accurate linear registration and motion correction of brain images. *NeuroImage*, **17**, 825–41.

Jones, R.M., Somerville, L.H., Li, J., *et al.* (2011). Behavioral and neural properties of social reinforcement learning. *Journal of Neuroscience*, **31**(37), 13039–45.

Jones, R.M., Somerville, L.H., Li, J., *et al.* (2014). Adolescent-specific patterns of behavior and neural activity during social reinforcement learning. *Cognitive, Affective & Behavioral Neuroscience*, **14**, 683–97.

Kendal, R.L., Boogert, N.J., Rendell, L., Laland, K.N., Webster, M., Jones, P.L. (2018). Social learning strategies: bridge-building between fields. *Trends in Cognitive Sciences*, 1–15.

Knoll, L.J., Leung, J.T., Foulkes, L., Blakemore, S.J. (2017). Age-related differences in social influence on risk perception depend on the direction of influence. *Journal of Adolescence*, **60**, 53–63.

Kucyi, A., Hove, M.J., Esterman, M., Hutchison, R.M., Valera, E.M. (2017). Dynamic brain network correlates of spontaneous fluctuations in attention. *Cerebral Cortex*, **27**, 1831–40.

Lane, S.T., Gates, K.M., Pike, H.K., Beltz, A.M., Wright, A.G.C. (2019). Uncovering general, shared, and unique temporal patterns in ambulatory assessment data. *Psychological Methods*, **24**, 54–69.

Lane, S.T., Gates, K.M. (2017). Automated selection of robust individual-level structural equation models for time series data. *Structural Equation Modeling*, **24**, 768–82.

Lin, L.C., Qu, Y., Telzer, E.H. (2018). Intergroup social influence on emotion processing in the brain. *Proceedings of the National Academy of Sciences*, 1–6.

Loewenstein, G.F., Hsee, C.K., Weber, E.U., Welch, N. (2001). Risk as feelings. *Psychological Bulletin*, **127**, 267–86.

Magee, J.C., Smith, P.K. (2013). The social distance theory of power. *Personality and Social Psychology Review*, **17**, 158–86.

Mather, M., Canli, T., English, T., *et al.* (2004). Amygdala responses to emotionally valenced stimuli in older and younger adults. *Psychological Science*, **15**, 259–63.

McCormick, E.M., van Hoorn, J., Cohen, J.R., Telzer, E.H. (2018). Functional connectivity in the social brain across childhood and adolescence. *Social Cognitive and Affective Neuroscience*, **13**, 819–30.

McCormick, E.M., Gates, K.M., Telzer, E.H. (2019). Model-based network discovery of developmental and performance-related differences during risky decision-making. *NeuroImage*, **188**, 456–64.

McCormick, E.M., Telzer, E.H. (2017). Adaptive adolescent flexibility: neurodevelopment of decision-making and learning in a risky context. *Journal of Cognitive Neuroscience*, **29**, 413–23.

McHale, S.M., Updegraff, K.A., Whiteman, S.D. (2012). Sibling relationships and influences in childhood and adolescence. *Journal of Marriage and Family*, **74**, 913–30.

Meldrum, R.C., Young, J.T.N., Weerman, F.M. (2012). Changes in self-control during adolescence: investigating the influence of the adolescent peer network. *Journal of Criminal Justice*, **40**, 452–62.

Morawetz, C., Bode, S., Baudewig, J., Heekeren, H.R. (2017). Effective amygdala-prefrontal connectivity predicts individual differences in successful emotion regulation. *Social Cognitive and Affective Neuroscience*, **12**, 569–85.

Nestler, S., Humberg, S. (2021). GIMME's ability to recover group-level path coefficients and individual-level path coefficients. *Methodology*, **17**, 58–91.

Op de Macks, Z.A., Flannery, J.E., Peake, S.J., *et al.* (2018). Novel insights from the Yellow Light Game: safe and risky decisions differentially impact adolescent outcome-related brain function. *NeuroImage*, **181**, 568–81.

Perino, M.T., Miernicki, M.E., Telzer, E.H. (2016). Letting the good times roll: adolescence as a period of reduced inhibition to appetitive social cues. *Social Cognitive and Affective Neuroscience*, **11**, 1762–71.

Pomery, E.A., Gibbons, F.X., Gerrard, M., Cleveland, M.J., Brody, G.H., Wills, T.A. (2005). Families and risk: prospective analyses of familial and social influences on adolescent substance use. *Journal of Family Psychology*, **19**, 560–70.

Qu, Y., Fuligni, A.J., Galvan, A., Telzer, E.H. (2015). Buffering effect of positive parent–child relationships on adolescent risk taking: a longitudinal neuroimaging investigation. *Developmental Cognitive Neuroscience*, **15**, 26–34.

Rhodes, G., Byatt, G., Michie, P.T., Puce, A. (2004). Is the fusiform face area specialized for faces, individuation, or expert individuation? *Journal of Cognitive Neuroscience*, **16**, 189–203.

Rogers, C.R., Perino, M.T., Telzer, E.H. (2020). Maternal buffering of adolescent dysregulation in socially appetitive contexts: from behavior to the brain. *Journal of Research on Adolescence*, **30**, 41–52.

Rogers, C.R., Lee, T.H., Fry, C.M., Telzer, E.H. (2021). Where you lead, I will follow: exploring sibling similarity in brain and behavior during risky decision making. *Journal of Research on Adolescence*, **31**, 34–51.

Rowe, D.C., Gulley, B.L. (1992). Sibling effects on substance use and delinquency*. *Criminology*, **30**(2), 217–34.

Samek, D.R., Goodman, R.J., Riley, L., McGue, M., Iacono, W.G. (2018). The developmental unfolding of sibling influences on alcohol use over time. *Journal of Youth and Adolescence*, **47**, 349–68.

Samek, D.R., Rueter, M.A. (2011). Associations between family communication patterns, sibling closeness, and adoptive status. *Journal of Marriage and Family*, **73**(5), 1015–31.

Schreuders, E., Braams, B.R., Blankenstein, N.E., Peper, J.S., Güroğlu, B., Crone, E.A. (2018). Contributions of reward sensitivity to ventral striatum activity across adolescence and early adulthood. *Child Development*, **89**, 797–810.

Schultz, R.T., Grelotti, D.J., Klin, A., *et al.* (2003). The role of the fusiform face area in social cognition: implications for the pathobiology of autism. *Philosophical Transactions of the Royal Society B: Biological Sciences*, **358**(1430), 415–27.

Silverman, M.H., Jedd, K., Luciana, M. (2015). Neural networks involved in adolescent reward processing: an activation likelihood estimation meta-analysis of functional neuroimaging studies. *NeuroImage*, **122**, 427–39.

Slomkowski, C., Rende, R., Conger, K.J., Simons, R.L., Conger, R.D. (2001). Sisters, brothers, and delinquency: evaluating social influence during early and middle adolescence. *Child Development*, **72**, 271–83.

Smith, A.R., Steinberg, L., Chein, J. (2014). The role of the anterior insula in adolescent decision making. *Developmental Neuroscience*, **36**, 196–209.

Smith., S.M. (2002). Fast robust automated brain extraction. *Human Brain Mapping*, **17**, 143–55.

Stephanou, K., Davey, C.G., Kerestes, R., *et al.* (2016). Brain functional correlates of emotion regulation across adolescence and young adulthood. *Human Brain Mapping*, **37**, 7–19.

Stormshak, E.A., Comeau, C.A., Shepard, S.A. (2004). The relative contribution of sibling deviance and peer deviance in the prediction of substance use across middle childhood. *Journal of Abnormal Child Psychology*, **32**, 635–49.

Telzer, E.H., van Hoorn, J., Rogers, C.R., Do, K.T. (2018). Social influence on positive youth development: A developmental neuroscience perspective. *Advances in Child Development and Behavior*, **54**, 215–58.

Tohka, J., Foerde, K., Aron, A.R., Tom, S.M., Toga, A.W., Poldrack, R.A. (2008). Automatic independent component labeling for artifact removal in fMRI. *NeuroImage*, **39**, 1227–45.

Tucker, C.J., McHale, S.M., Crouter, A.C. (2001). Conditions of sibling support in adolescence. *Journal of Family Psychology*, **15**, 254–71.

Uddin, L.Q. (2015). Salience processing and insular cortical function and dysfunction. *Nature Reviews Neuroscience*, **16**, 55–61.

van Hoorn, J., van Dijk, E., Meuwese, R., Rieffe, C., Crone, E.A. (2014). Peer influence on prosocial behavior in adolescence. *Journal of Research on Adolescence*, **26**, 90–100.

van Hoorn, J., Shablack, H., Lindquist, K.A., Telzer, E.H. (2019). Incorporating the social context into neurocognitive models of adolescent decision-making: a neuroimaging meta-analysis. *Neuroscience and Biobehavioral Reviews*, 1–14.

Welborn, B.L., Lieberman, M.D., Goldenberg, D., Fuligni, A.J., Galván, A., Telzer, E.H. (2016). Neural mechanisms of social influence in adolescence. *Social Cognitive and Affective Neuroscience*, **11**, 100–9.

Whiteman, S.D., McHale, S.M., Crouter, A.C. (2007). Competing processes of sibling influence: observational learning and sibling deidentification. *Social Development*, **16**, 642–61.

Whiteman, S.D., Bernard, J.M.B., Mchale, S.M. (2010). The nature and correlates of sibling influence in two-parent African American families. *Journal of Marriage and Family*, **72**, 267–81.

Whiteman, S.D., McHale, S.M., Soli, A. (2011). Theoretical perspectives on sibling relationships. *Journal of Family Theory & Review*, **3**, 124–39.

Whiteman, S.D., Zeiders, K.H., Killoren, S.E., Rodriguez, S.A., Updegraff, K.A. (2014). Sibling influence on Mexican-origin adolescents' deviant and sexual risk behaviors: the role of sibling modeling. *The Journal of Adolescent Health*, **54**, 587–92.

Yurasek, A.M., Brick, L., Nestor, B., Hernandez, L., Graves, H., Spirito, A. (2018). The effects of parent, sibling and peer substance use on adolescent drinking behaviors. *Journal of Child and Family Studies*, **28**, 73–83.

Zerubavel, N., Bearman, P.S., Weber, J., Ochsner, K.N. (2015). Neural mechanisms tracking popularity in real-world social networks. *Proceedings of the National Academy of Sciences*, **112**, 15072–7.